Enhancing COVID-19 Diagnosis with Deep Learning Models DenseNet and ResNet on Medical Imaging Data

S. Chowdri[1], S. Shanthi[1], R. Dhanaeswaran[1], P. Giridar Prasad[1], K. Nirmala Devi[1] and A. Kavitha[2]

[1]*Dept. of Computer Science and Engineering, Kongu Engineering College, Erode, India*

[2]*Dept. of Computer Science and Engineering, Government College of Engineering (IRTT), Erode, India*

Keywords: Covid-19 Diagnosis, Deep Learning, DenseNet, ResNet, CT Scan, Chest X-Ray, Image Classification, Accuracy.

Abstract: The COVID-19 pandemic has put immense pressure on health systems worldwide. Early and accurate diagnosis is thus an important modality of management of the disease. RT-PCR tests are the gold standard for diagnosis but suffer from a number of limitations such as high processing time and occasional false negatives. Diagnostic imaging via chest X rays and CT scans offers a rapid, non-invasive alternative for detecting COVID-19-induced lung abnormalities. This study evaluates the performance of various configurations of DenseNet (121, 169, 201) and ResNet-152 for automated COVID-19 detection using chest X-rays and CT scans. More in particular, DenseNet-201 yielded a good result of approximately 96% accuracy for CT scans and 99% for X-rays when trained with the Adam optimizer using a batch size of 32. It highlights that the choice of optimizer and batch size has paramount importance. DenseNet-201's efficient gradient flow, feature reuse, and parameter utilization make it especially suitable for medical imaging applications with limited annotated datasets. Its robust feature extraction capabilities position it as a reliable diagnostic tool, potentially enhancing clinical workflows and accelerating COVID-19 diagnosis. This study underscores DenseNet-201's potential to improve patient outcomes and pandemic management through accurate, automated medical image analysis.

1 INTRODUCTION

COVID-19 is a disease that appeared suddenly at the end of 2019, caused by the virus SARS-CoV-2, and has since caused huge destruction to the health, economies, and daily life of the world. It is transmitted by aerosols, droplets, contaminated surfaces, and air. The symptoms range from very mild to the most severe and can involve fever, cough, difficulty breathing, severe problems in the lungs, organ failure, and, in extreme cases, death. For example, the Delta and Omicron variants spread so quickly because of their high contagion rate, sometimes for evading immunity. This is not mentioning the vaccine coverage that was reached or the lingering effects that many people were still battling against COVID-19 in mid-2024.Conventional medical imaging represents another field where CNNs revolutionized the way it presents unparalleled capabilities for the detection, segmentation, and classification of different image classes.

It is of great help in diagnosing diseases of the lungs, such as lung cancer, tuberculosis, and pneumonia, all at once. During the pandemic period of COVID-19, CNNs became important for researching chest X-ray features along with computed tomography. The specialty in architectures of CNN comes forth through ResNets and VGG, and then further Inception, aside from others. Each of them is unique and has its particular power, like residual connections and skip connections in ResNet networks, which enable the training of deeper networks; making simpler designs boosts feature learning in VGG, while Inception further improves this with its two most innovative connectivity ideas: convolutional blocks on several parallel branches with concatenated feature maps. It allows every layer to directly feed into all previous ones, encourages feature reuse, and makes the flow of gradients better. This architecture will learn both low-level and high-level features for finding subtle abnormalities in a medical image.The efficiency and resistance to overfitting make

Chowdri, S., Shanthi, S., Dhanaeswaran, R., Giridar Prasad, P., Devi, K. N. and Kavidha, A.
Enhancing COVID-19 Diagnosis with Deep Learning Models DenseNet and ResNet on Medical Imaging Data.
DOI: 10.5220/0013595700004664

In *Proceedings of the 3rd International Conference on Futuristic Technology (INCOFT 2025) - Volume 2*, pages 506-513
ISBN: 978-989-758-763-4

DenseNet very relevant to high-dimensional data associated with medical applications. Most of the recent works on COVID-19 diagnostics, tumor segmentation, skin lesion detection, and diabetic retinopathy classification have been based on this approach. Compared to ResNet and VGG models, DenseNet is more parameter-efficient with high accuracy and fewer parameters, hence having less risk of overfitting. This is of extreme value in providing accurate diagnoses in resource-poor settings. This would, in turn, enable the radiologists to provide accurate and reproducible results on well-preprocessed and well-annotated datasets with significantly less workload. Its performance can be improved by performing hyperparameter tuning, with evaluation metrics such as accuracy and AUC-ROC. DenseNet bridges advanced AI technology with practical healthcare applications; thus, it holds tremendous potential to revolutionize diagnostics and support clinicians worldwide in combating COVID-19 and other diseases.

2 LITERATURE REVIEW

A study designed a CAD system that classified chest X- rays into COVID-19 pneumonia, other pneumonia, and normal cases using transfer learning -based CNN following the use of preprocessing techniques like removal of the diaphragm region and histogram equalization(A. T, S. S, N. K, A. K, D. R. B and N. Rajkumar, Sentiment Analysis on Covid-19 Data Using BERT Model, 2024 International Conference on Advances in Modern Age Technologies for Healt, n.d.) (Nirmala Devi, K., Shanthi, S., Hemanandhini, K., Haritha, S., Aarthy, S. (2022). Analysis of COVID-19 Epidemic Disease Dynamics Using Deep Learning. In Kim, J.H., Deep, K., Geem, Z.W., Sadollah, A., Yadav, A. (Eds) Proceed, n.d.).The model achieved an accuracy of 94. 5% on a dataset of 8,474 images and reported that the performance was enhanced significantly with the use of preprocessing techniques and revealed how significant image enhancement is towards the achievement of better performance in COVID-19 detection (Heidari et al., 2020). The analysis of deep learning models to identify COVID- 19 from chest X-rays on a dataset of 5,000 images showed the four CNNs that were part of the experiment, including ResNet18, ResNet50, SqueezeNet, and DenseNet-121, achieving a 98% sensitivity rate and a 90% specificity rate after transfer learning training. Precision in high lighting the infected lung regions of COVID-19 was observed in the heatmaps generated by the models while matching with the annotations made by the radiologists. The results are promising, but the study points out that larger datasets need to be created for even more reliable accuracy assessments (Minaee et al., 2020). ACoS is an abbreviation for Automatic COVID Screening system in this study which is the classification of patients into normal, suspected, and infected with COVID 19 using radiomic texture descriptors from chest X-rays. The ensemble uses a majority 3 voting of five supervised classifiers in a two- phase classification approach. The validation was performed using 258 images with an accuracy of 98. 06% in the first phase (normal vs. abnormal) and 91. 33% in the second phase (pneumonia vs. COVID-19). The obtained results manifested a statistical difference and even surpassed some of the techniques currently used for COVID-19 detection (Chandra et al., 2021). A recent study presents a Deep Convolutional Neural Network (CNN)-based approach for the detection of COVID-19 from chest X-ray images. Models used in this solution are DenseNet201, ResNet50V2, and Inceptionv3, which are specifically trained and then combined using a weighted average ensembling. With 538 images positive for COVID-19 and 468 negative images for COVID-19, the model was able to achieve a classification accuracy of 91.62%. In addition, the study created an intuitive graphical user interface application to make medical practitioners quickly detect the existence of COVID-19 in the chest X-ray images (Das et al., 2021). A study proved that AI can be used to automate and improve the detection accuracy for COVID-19 using Chest X-ray (CXR) and CT images. Besides, AI can be also utilized in DL techniques such as Convolutional Neural Networks (CNN). This paper dis cusses research works on this topic, challenges, and recent breakthroughs on the DL based classification of COVID-19. The review also suggests further research that should further improve the performance and reliability of automated systems for COVID-19 image classification (Aggarwal et al., 2022). An article classifies COVID-19 patient individuals using chest X-ray scans and com pares various CNN models that base their work on deep learning. In this, a dataset consisting of 6432 samples from the Kaggle repository was tested using data augmentation with Xception, ResNeXt, and Inception V3. It was seen that among these, Xception is having the highest accuracy as 97. 97%. The findings of the analysis are not medical but show that automated deep learning techniques might be useful for the screening of COVID-19 patients (Jain et al., 2021). To overcome the deficiencies of previous networks, a paper proposed a dual path way, 11-layer deep 3D

Convolutional Neural Network for the segmentation of brain lesions. It fused an efficient dense training scheme with a dual pathway architecture that computes multi-scale input. The proposed approach demonstrated superior performance on benchmarking BRATS 2015 and ISLES 2015 experiments in multi-channel MRI data of ischemic stroke, brain tumors, and traumatic brain injuries. The method is found to be effective and computationally efficient and thus suitable for research as well as clinical applications (Kamnitsas et al., 2017). It performed an experiment using Transfer Learning to evaluate the state-of-the-art convolutional neural networks on X-ray images from patients infected with COVID 19, bacterial pneumonia, and normal conditions. Based on the study, the Deep Learning models were shown to detect COVID-19 with as high as 96. 78% accuracy, 98. 66% 4 sensitivity, and 96. 46% specificity. Results indicate that X- ray imaging could be an important step toward the diagnosis of COVID-19; thus, more research needs to be done in the medical field (Apostolopoulos & Mpesiana, 2020). A research introduced COVID-CAPS, a model of capsule network for the substitution of CNN diagnosis in COVID-19 using X-ray images. Compared to the previously designed CNN model, COVID-CAPS reported to have an accuracy of 95. 7%, sensitivity of 90%, and specificity of 95. 8%, which solved most drawbacks. These included small amounts of sample data and loss of spatial information in CNNs. It is promising as a diagnostic tool for COVID-19, as further improvement to 98.3% accuracy and 98.6% specificity was achieved by pre-training with an X-ray image dataset (Afshar et al., 2020). A study designed clinical predictive models for the identification of COVID-19 cases based on laboratory data and deep learning. It tested these models on data from 600 patients, with an impressive accuracy of 86. 66%, F1-score of 91. 89%, and a recall of 99. 42%. The implications are that these clinical predictive models may help the medical professional validate the reliability of results from laboratories and efficiently use resources during the pandemic (Alakus & Turkoglu, 2020)

3 EXPERIMENTAL SETUP

3.1 Dataset

3.1.1 CT Scan

This dataset was downloaded from Kaggle, "COVID-19 CT Scan Dataset" by Dr. Surabhi Thorat, and it consists of COVID and Non-COVID images, which are well-labeled, hence perfect for training diagnostic machine learning models. Images were then split into two categories: COVID-19 and Non-COVID combined into a single DataFrame for easy manipulation, then stratified into an 80:20 training-validation split of 6095 training and 1525 validation. Stratification has ensured that both categories are well represented, hence the integrity of the data is maintained without bias during model training and validation.

3.1.2 X Ray

The dataset used in this research has been curated by Prashant from Kaggle and is titled "Chest X-ray (COVID-19 & Pneumonia)". The dataset comprises a collection of X-ray images of cases related to COVID-19, pneumonia, and healthy ones. In this work, cases of pneumonia are not taken into consideration, hence, the classes considered for analysis are COVID-19 and Non- COVID. In all, the dataset holds 2,159 images. It is split into an 80:20 stratified split for 1,726 training samples and 433 validation samples that maintain a balanced class representation. Label them, categorize the images as COVID-19 and Non-COVID, and merge them into one DataFrame to accelerate the processing that can later be easily split with the assurance that this would maintain the integrity of the data and representativity of the sets for a proper training and validation process.

3.2 Data Augmentation

To enhance the generalization ability of our models and compensate for the relatively limited size of the dataset, various data augmentation techniques were employed. These included:

Table 1: Data Augmentation Techniques.

Augmentation Technique	Description
Rotation Range	Rotates images randomly within the specified degree range.
Width Shift Range	Randomly shifts images horizontally by a specified fraction.
Height Shift Range	Randomly shifts images vertically by a specified fraction.
Shear Range	Applies random shearing transformations to the images.
Zoom Range	Randomly zooms in or out on images.
Horizontal Flip	Randomly flips images horizontally.
Rescale	Normalizes pixel values by scaling them by specified factor.

3.3 Model Architecture

Traditional CNNs have sequential information flow, from one layer to the next. However, in DenseNet every layer receives input from all preceding layers and passes its own feature maps to all subsequent layers. So, the i-th layer receives feature maps of all the previous layers,

$$x0, x1, x2, \ldots xl-1, \qquad as\ input:$$

$$x1 = H1([x0, x1, x2, \ldots\ldots, xl-1]) \qquad (1)$$

where H1 is a composite function of batch normalization, ReLU and convolution. Dense connectivity leads to the +following benefits: Direct connections between layers would allow gradients to flow more easily in the backwards propagation pass so as to mitigate the problem of vanishing gradients. Layers could read the feature maps of all preceding layers, so reuse of features is encouraged and redundancy is reduced. This architecture uses fewer parameters than its traditional counterparts at the same depth due to the fact that it does not have to learn redundant feature maps in the first place.

A Dense Net consists of several dense blocks. The dense block itself comprises multiple convolutional layers, which are connected densely. Between the dense blocks, transition layers are provided to carry out the down sampling operations and decrease the spatial dimensions of the feature maps. Dense Block: It is a sequence of layers wherein each layer is fed forward to every other layer. Each layer feature maps are concatenated with all inputs from the following layers. Transition Layer: It lies between the dense blocks. It utilizes a 1x1 convolution to compress features, followed by feature map reducing a 2x2 average pooling operation along with batch normalization. Dense Net exists in many configurations that are primarily different in depth, concerning the number of layers. Currently, three variants are widely used, such as DenseNet121, DenseNet169, and DenseNet201.

Here, each number corresponds to the total quantity of the layers inside the network, counting both convolutional, pooling, and fully connected layers.

Table 2: Comparison between Traditional CNN and DenseNet.

Feature	Traditional CNN	DenseNet
Connectivity	Sequential	Dense (each layer connected to all previous layers)
Gradient Flow	Can be hindered by depth (vanishing gradient)	Improved due to direct connections
Feature Reuse	Limited	Extensive
Parameter Efficiency	Higher due to redundant feature maps	Lower, more efficient

3.3.1 DenseNet 121

It has 121 layers. It offers an excellent balance between depth and computational efficiency and best applicable in places where computation is much needed.

3.3.2 DenseNet 169

It adds to the architecture through adding more layers, therefore giving depth for feature extraction when the complexity goes up a notch. This variation is very good for tasks which need the recognition of fine details and is computationally costly.

3.3.3 DenseNet 201

Being one of the deepest variants, with a count of 201 layers, it provides the finest feature extraction capability. In particular, it is well-suited for more complex applications but with huge computational and memory resource requirement

3.3.4 ResNet 152

ResNet-152 deep learning model was designed to solve problems with the vanishing gradient in deep neural networks. The gradients can flow through shortcut connections that bypass layers. It is built from residual blocks with two or three convolutional layers, with batch normalization and ReLU for activation. These shortcut connections add the input of the block directly to the output, hence enabling the network to learn residual functions. ResNet-152 is a 152-layer network with about 60.2 million parameters. An architecture so deep, trained efficiently for very deep networks, improves the accuracy and performance on many tasks like image classification and medical image analysis

Layers	Output Size	DenseNet-121	DenseNet-169	DenseNet-201
Convolution	112×112	7×7 conv, stride 2		
Pooling	56×56	3×3 max pool, stride 2		
Dense Block (1)	56×56	$\begin{bmatrix} 1 \times 1 \text{ conv} \\ 3 \times 3 \text{ conv} \end{bmatrix} \times 6$	$\begin{bmatrix} 1 \times 1 \text{ conv} \\ 3 \times 3 \text{ conv} \end{bmatrix} \times 6$	$\begin{bmatrix} 1 \times 1 \text{ conv} \\ 3 \times 3 \text{ conv} \end{bmatrix} \times 6$
Transition Layer (1)	56×56	1×1 conv		
	28×28	2×2 average pool, stride 2		
Dense Block (2)	28×28	$\begin{bmatrix} 1 \times 1 \text{ conv} \\ 3 \times 3 \text{ conv} \end{bmatrix} \times 12$	$\begin{bmatrix} 1 \times 1 \text{ conv} \\ 3 \times 3 \text{ conv} \end{bmatrix} \times 12$	$\begin{bmatrix} 1 \times 1 \text{ conv} \\ 3 \times 3 \text{ conv} \end{bmatrix} \times 12$
Transition Layer (2)	28×28	1×1 conv		
	14×14	2×2 average pool, stride 2		
Dense Block (3)	14×14	$\begin{bmatrix} 1 \times 1 \text{ conv} \\ 3 \times 3 \text{ conv} \end{bmatrix} \times 24$	$\begin{bmatrix} 1 \times 1 \text{ conv} \\ 3 \times 3 \text{ conv} \end{bmatrix} \times 32$	$\begin{bmatrix} 1 \times 1 \text{ conv} \\ 3 \times 3 \text{ conv} \end{bmatrix} \times 48$
Transition Layer (3)	14×14	1×1 conv		
	7×7	2×2 average pool, stride 2		
Dense Block (4)	7×7	$\begin{bmatrix} 1 \times 1 \text{ conv} \\ 3 \times 3 \text{ conv} \end{bmatrix} \times 16$	$\begin{bmatrix} 1 \times 1 \text{ conv} \\ 3 \times 3 \text{ conv} \end{bmatrix} \times 32$	$\begin{bmatrix} 1 \times 1 \text{ conv} \\ 3 \times 3 \text{ conv} \end{bmatrix} \times 32$
Classification Layer	1×1	7×7 global average pool		
		1000D fully-connected, softmax		

Figure 1: Differentiation of layers between DenseNet Architectures.

3.4 Methodology

This paper uses the complete dataset of COVID-19 X-ray and CT-scan images downloaded from Kaggle for training and testing machine learning models for diagnosis. A variety of DenseNet architecture variants, including DenseNet-101, DenseNet-121, and DenseNet-201, are considered along with ResNet for the analysis using transfer learning techniques. Transfer learning was applied by initializing the weights of DenseNet pre-trained on ImageNet. This ensured that the starting point for our models was considerably robust and had leveraged some of the rich feature representations learned from a diverse set of images. The dataset was well-structured, split roughly 80-20 between training and validation sets; this helps prevent bias and maintains integrity in the dataset by ensuring that the distribution of COVID-19 and non-COVID-19 images remains constant across both sets. Accordingly, early stopping during training kept a constant eye on the model's performance on the validation set and stopped it when it saw it did not improve anymore. In that way, this technique avoids overfitting; by doing so, it keeps the model generalizing even to new data fed into it. Each of these trained models was then comprehensively evaluated against different metrics, namely AUC-ROC, accuracy, specificity, recall, and precision. AUC-ROC expresses the measure of how well the model is capable of distinguishing between classes, while accuracy is the general correctness of the predictions made by the model. Specificity will explain how well the model provides the true negatives, and recall will provide the performance of identifying true positives. Precision provided a view into how well that model identified true positives among all that were predicted as positive.

3.5 Training And Optimisation

In this work, transfer learning is adopted by initializing the DenseNet models with pre-trained weights from ImageNet. In that way, the DNNs will leverage the rich feature representations they have learned on such a large and diverse dataset for fast convergence and improvement in performance toward the COVID-19 diagnosis task. In training, the base layers in DenseNet were frozen in order to maintain all the valuable pre-trained features while training the head for classification, for adapting it to our binary classification task. The custom head consists of a global average pooling layer followed by fully connected layers, culminating in a sigmoid activation that outputs class probabilities using the loss function as Binary cross-entropy.

The DenseNet is densely connected; this aids in better gradient flow and feature propagation, which can be of great help for such complex tasks as medical image classification. An optimization of the model performance was basically carried out with the Adam optimizer because it has an adaptive learning rate and it is efficient in handling sparse gradients, which helps speed up the convergence.

However, in order to really assess model performance, further exploration of the models with different optimizers is intended, including RMSprop, SGD, and Adam, along with various batch sizes. Each of these optimizers has its merits: Adam is adaptive with its learning rates but sometimes converges to suboptimal solutions; SGD offers better generalization but needs careful tuning and may result in slow convergence; and RMSprop acts best on non-stationary problems, though it can converge more slowly than Adam on deeper networks.

Table 3: Model Architecture.

Component	Description
Global Average Pooling	Reduces spatial dimensions of feature maps
Dense Layer (ReLu)	Adds non-linearity and enhances learning
Output Layer (Sigmoid)	Binary output for classification

Batch size does play an important role while training a model. Larger batch size provides smoother estimates of gradient, faster convergence, requires a lot of memory, though carries the risk of trapping into a local minimum; smaller batch size introduces extra noise into the gradient estimation. This might help the models from escaping local minima with somewhat slow convergence. We systematically try these various optimizers and batch sizes in order to see what the best combination of the two might be that yields better performance for our particular classification problem.

4 RESULT AND DISCUSSION

Table 4: Accuracy for DenseNet121 for CT SCAN Dataset.

Optimizer	Batch Size(16)	Batch Size(32)	Batch Size(64)
Adam	94. 75	95. 50	94. 20
RMSprop	93. 85	94. 30	93. 10
SGD	92. 60	93. 50	92. 00

Table 5: Accuracy for DenseNet169 for CT SCAN Dataset

Optimizer	Batch Size(16)	Batch Size(32)	Batch Size(64)
Adam	95. 20	94. 50	92. 80
RMSprop	94. 00	93. 50	91. 50
SGD	89. 80	88. 50	86. 70

Table 6: Accuracy for DenseNet201 for CT SCAN Dataset.

Optimizer	Batch Size(16)	Batch Size(32)	Batch Size(64)
Adam	94. 00	96. 90	95. 70
RMSprop	94. 50	96. 10	95. 10
SGD	93. 30	95. 20	94. 30

Table 7: Accuracy for ResNet152 for CT SCAN Dataset.

Optimizer	Batch Size(16)	Batch Size(32)	Batch Size(64)
Adam	94. 50	95. 70	94. 00
RMSprop	92. 80	93. 50	92. 10
SGD	91. 80	92. 20	90. 50

Comparing all different models, namely DenseNet-121, DenseNet-169, DenseNet-201, and ResNet-152, with a set of different optimizers and batch sizes, it can be found that the best results come out to be from DenseNet-201. With the Adam optimizer and batch size of 32, this has achieved an accuracy of 96.9%. Relatively, one more working combination for the DenseNet-201 model was with RMSprop as the optimizer and a batch size of 32, which yielded the same result of 96.1% accuracy. The best after that is DenseNet-121, which reaches a peak of 95.5% with the Adam optimizer and batch size 32. Next comes DenseNet-169, which, compared to its other variants, reached a peak of 95.2% with the Adam optimizer and batch size of 16. ResNet-152 was competitive but reached a peak of 95.7% only at the Adam optimizer with a batch size of 32. Therefore, in all models, the best performance was obtained when, for the Adam optimizer, the batch size was set to 32. Thus, it is the best configuration. On the other hand, DenseNet-201 yielded the best performance on the Covid-19 CT-scan dataset when using Adam with a batch size of 32.

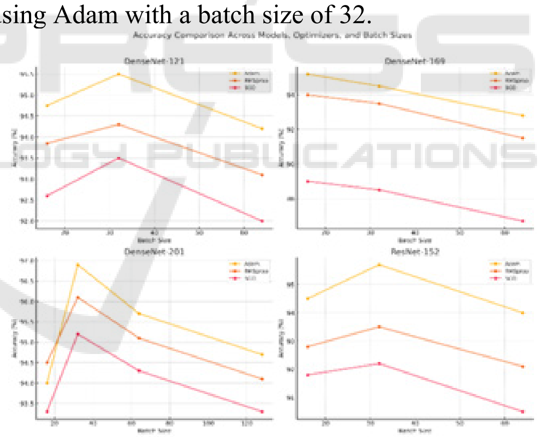

Figure 2: Comparison of various DenseNet and ResNet Architectures for CT scan Dataset.

Table 8: Accuracy for DenseNet121 for X Ray Dataset.

Optimizer	Batch Size(16)	Batch Size(32)	Batch Size(64)
Adam	97. 85	98. 50	98. 20
RMSprop	97. 70	98. 00	97. 85
SGD	96. 50	97. 00	96. 70

Table 9: Accuracy for DenseNet169 for X Ray Dataset.

Optimizer	Batch Size(16)	Batch Size(32)	Batch Size(64)
Adam	96. 70	98. 20	97. 30
RMSprop	95. 90	97. 50	96. 50
SGD	94. 50	96. 20	95. 00

Table 10: Accuracy for DenseNet201 for X Ray Dataset.

Optimizer	Batch Size(16)	Batch Size(32)	Batch Size(64)
Adam	98. 90	99. 30	98. 95
RMSprop	98. 30	98. 85	98. 50
SGD	97. 50	98. 20	97. 80

Table 11: Accuracy for ResNet152 for X Ray Dataset.

Optimizer	Batch Size(16)	Batch Size(32)	Batch Size(64)
Adam	94. 50	95. 20	94. 00
RMSprop	93. 70	94. 50	93. 20
SGD	92. 50	93. 00	91. 80

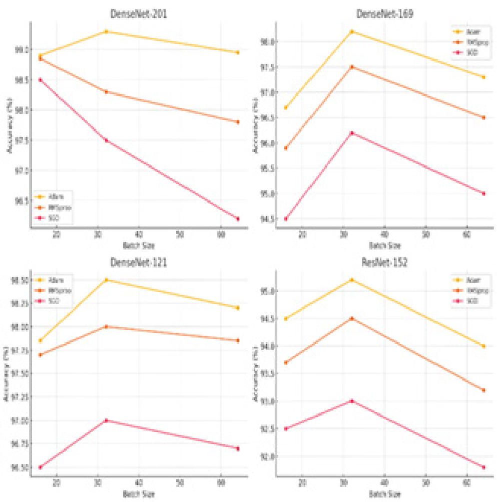

Figure 3: Comparison of various DenseNet and ResNet Architectures for X-ray Dataset.

A comparison of the accuracies attained for the various models using the X-ray dataset shows that the highest, from DenseNet-201 with the Adam optimizer and batch size of 32, was 99.30%. This is closely followed by DenseNet-121, which had attained an accuracy of 98.50% under the same conditions and consistently showed quite good performance under other batch sizes and optimizers. Among these, DenseNet-169 had the highest accuracy of 98.20% with the Adam optimizer and batch size 32, ranking slightly after the top two. ResNet-152 is a little lagging and achieved a maximum of 95.70% accuracy under similar settings. Hence, DenseNet-201 and DenseNet-121 are the best models for this dataset, especially with the Adam optimizer and batch size 32, predestining these models for X-ray image classification tasks.

ACKNOWLEDGEMENTS

The author acknowledges AICTE for providing the fund for conducting this research. AICTE, the reference no. F.No.8-80/FDC/RPS/POLICY-1/2021-22/ Dated: 18.02.2022.

REFERENCES

A. T, S. S, N. K, A. K, D. R. B and N. Rajkumar, Sentiment Analysis on Covid-19 data Using BERT Model, 2024 International Conference on Advances in Modern Age Technologies for Healt. (n.d.).

Afshar, P., Heidarian, S., Naderkhani, F., Oikonomou, A., Plataniotis, K. N., & Mohammadi, A. (2020). COVID-CAPS: A capsule network-based framework for identification of COVID-19 cases from X-ray images. Pattern Recognition Letters, 138, 638–643. https://doi.org/10.1016/J.PATREC.2020.09.010

Aggarwal, P., Mishra, N. K., Fatimah, B., Singh, P., Gupta, A., & Joshi, S. D. (2022). COVID-19 image classification using deep learning: Advances, challenges and opportunities. Computers in Biology and Medicine, 144, 105350. https://doi.org/10.1016/J.COMPBIOMED.2022.105350

Alakus, T. B., & Turkoglu, I. (2020). Comparison of deep learning approaches to predict COVID-19 infection. Chaos, Solitons & Fractals, 140, 110120. https://doi.org/10.1016/J.CHAOS.2020.110120

Apostolopoulos, I. D., & Mpesiana, T. A. (2020). Covid-19: automatic detection from X-ray images utilizing transfer learning with convolutional neural networks. Physical and Engineering Sciences in Medicine, 43(2), 635–640. https://doi.org/10.1007/s13246-020-00865-4

Chandra, T. B., Verma, K., Singh, B. K., Jain, D., & Netam, S. S. (2021). Coronavirus disease (COVID-19) detection in Chest X-Ray images using majority voting based classifier ensemble. Expert Systems with Applications, 165, 113909. https://doi.org/10.1016/J.ESWA.2020.113909

Das, A. K., Ghosh, S., Thunder, S., Dutta, R., Agarwal, S., & Chakrabarti, A. (2021). Automatic COVID-19 detection from X-ray images using ensemble learning with convolutional neural network. Pattern Analysis and Applications, 24(3), 1111–1124. https://doi.org/10.1007/s10044-021-00970-4

Heidari, M., Mirniaharikandehei, S., Khuzani, A. Z., Danala, G., Qiu, Y., & Zheng, B. (2020). Improving the performance of CNN to predict the likelihood of COVID-19 using chest X-ray images with preprocessing algorithms. International Journal of Medical Informatics, 144, 104284. https://doi.org/10.1016/J.IJMEDINF.2020.104284

Jain, R., Gupta, M., Taneja, S., & Hemanth, D. J. (2021). Deep learning based detection and analysis of COVID-19 on chest X-ray images. Applied Intelligence, 51(3), 1690–1700. https://doi.org/10.1007/s10489-020-01902-1

Kamnitsas, K., Ledig, C., Newcombe, V. F. J., Simpson, J. P., Kane, A. D., Menon, D. K., Rueckert, D., & Glocker, B. (2017). Efficient multi-scale 3D CNN with fully connected CRF for accurate brain lesion segmentation. Medical Image Analysis, 36, 61–78. https://doi.org/10.1016/J.MEDIA.2016.10.004

Minaee, S., Kafieh, R., Sonka, M., Yazdani, S., & Jamalipour Soufi, G. (2020). Deep-COVID: Predicting COVID-19 from chest X-ray images using deep transfer learning. Medical Image Analysis, 65, 101794. https://doi.org/10.1016/J.MEDIA.2020.101794

Nirmala Devi, K., Shanthi, S., Hemanandhini, K., Haritha, S., Aarthy, S. (2022). Analysis of COVID-19 Epidemic Disease Dynamics Using Deep Learning. In Kim, J.H., Deep, K., Geem, Z.W., Sadollah, A., Yadav, A. (eds) Proceed. (n.d.).